Research Article Vol. 27, No. 11 | 27 May 2019 | OPTICS EXPRESS 15283

Optics EXPRESS

Cascaded sum-frequency generation and electro-optic polarization coupling in the PPLNOI ridge waveguide

DAN WANG,[1,2] TINGTING DING,[1,2] YUANLIN ZHENG,[1,2,3] AND XIANFENG CHEN[1,2,4]

[1] *State Key Laboratory of Advanced Optical Communication Systems and Networks, School of Physics and Astronomy, Shanghai Jiao Tong University, Shanghai 200240, China*
[2] *Key Laboratory for Laser plasma (Ministry of Education), Collaborative Innovation Center of IFSA (CICIFSA), Shanghai Jiao Tong University, Shanghai 200240, China*
[3] *ylzheng@sjtu.edu.cn*
[4] *xfchen@sjtu.edu.cn*

Abstract: Quasi-phase matched sum-frequency generation (SFG) and electro-optic (EO) polarization coupling has been realized simultaneously in a periodically poled lithium niobate on insulator (PPLNOI) ridge waveguide. Therefore, utilizing the cascading process, the intensity of sum-frequency conversion can be modulated by applying a transverse electric field. The driving voltage is reduced by using the ridge waveguide structure, and also the frequency conversion efficiency is enhanced. This scheme is proposed to control nonlinear frequency conversion by electric field applying on the lithium niobate on insulator (LNOI) platform. The integration and fast-speed modulation of the configuration may find applications in nonlinear optical processing and communication.

1. Introduction

Cascading processes have extensive applications in optics which benefits a lot from their enhancement ability and versatile configuration as compared with direct ones. The most recognized example is that through cascaded second-order optical nonlinearities one can obtain an effective large enhancement of third-order nonlinearity [1–3]. The two key features of this cascading process are the existence of nonlinear phase shifts and optical solitons [4, 5]. This has wide applications in three-wave mixing, spatial non-reciprocity, pulse compression and optical bistability [6–8]. For instance, cascaded sum-frequency generation (SFG) and difference frequency generation (DFG) aiming for multiwavelength frequency conversion plays an important role in all-optical switching and wavelength division multiplexing systems [9]. Besides, cascaded linear electro-optic (EO) effect has been proposed as an analogy of cascaded second-order nonlinearity which can enhance the Kerr EO effect in noncentrosymmetric crystals. The scheme has applications in phase control [10, 11].

Traditional methods to control nonlinear processes, e.g. temperature control and angle adjustment, are inflexible and slow in response. Cascaded frequency conversion and EO effect can modulate the nonlinear process via an applied electric field. The nonlinear frequency conversion controlled by electric field is intrinsically fast, reliable and convenient [12]. In the past few years, research related to cascade second-harmonic generation (SHG) and EO polarization coupling has been intensively carried out [13–15]. Cascaded linear EO effect induces nonlinear phase shift to generate a large effective nonlinear refractive index, and further influences the phase mismatching of SHG. Hence, the intensity and polarization of second-harmonic can be easily modulated by the applied electric field. But there are some crucial issues in previous methods. On one hand, the cascading process based on bulk media is inefficient in both frequency

#362822 https://doi.org/10.1364/OE.27.015283
Journal © 2019 Received 20 Mar 2019; revised 2 May 2019; accepted 2 May 2019; published 13 May 2019

conversion and electric field applying. On the other hand, the QPM conditions of SHG and EO polarization coupling only occurs at one critical condition [13, 14, 16]. This limitation fixes the operating wavelength of the cascading process and the critical condition is also hard to satisfy in many practical applications. Here, we propose a new scheme to address these issues by utilizing the cascading of SFG and EO polarization coupling, which shows both electrically controlled nonlinear conversion and flexible operational wavelengths.

Here, integration of cascaded SFG and EO polarization coupling is experimentally investigated in a periodically poled lithium niobate on insulator (PPLNOI) ridge waveguide on the micrometer-thick lithium niobate on insulator (LNOI) platform. Quasi-phase matching (QPM) based on periodically domain-engineered structures in the nonlinear crystal is employed for effective nonlinear frequency conversion. The structure of LNOI ridge waveguide dramatically enhances both the nonlinear and EO effects. The integrated device represents a kind of electrically controlled nonlinear photonic functionality for fast-speed, low-voltage, and low input power [17–19]. More than that, cascaded SFG and EO polarization coupling shows better flexibility and adjustability, because the QPM conditions of SFG and EO effects are relatively independent.

2. Theoretical model

The cascaded SFG and EO polarization coupling process can be modeled using coupled-wave equations, assuming plane wave approximation and that effective refractive indices be taken into account in the ridge waveguide structure. Considering the case in PPLN, two fundamental pump waves, denoted as FF_1^e and FF_2^e with the superscript representing its polarization state, propagates along the x direction. The polarization of the two waves are both along z axis to use the largest second-order nonlinear coefficient d_{33}. Sum-frequency wave (SF^e) is generated under type-0 QPM condition. Let FF_1^e also satisfy the QPM condition of transverse EO polarization coupling. This is achievable in PPLN with one single poling period in the telecom band. The coupled equations governing the SFG and EO polarization coupling processes ($FF_1^e + FF_2^e \rightarrow SF^e, FF_1^e \rightarrow FF_1^o$) can be derived as follows [13–15]:

$$\frac{dE_{1z}}{dx} = -i\frac{\omega_1}{2n_{1z}c}\left(\beta(x)E_{1y}e^{-i\Delta k_{EO}x} + 2d(x)E_{2z}^*E_{3z}e^{-i\Delta k_{SFG}x}\right), \quad (1)$$

$$\frac{dE_{1y}}{dx} = -i\frac{\omega_1}{2n_{1y}c}\beta(x)E_{1z}e^{i\Delta k_{EO}x}, \quad (2)$$

$$\frac{dE_{2z}}{dx} = -i\frac{\omega_2}{n_{2z}c}d(x)E_{1z}^*E_{3z}e^{-i\Delta k_{SFG}x}, \quad (3)$$

$$\frac{dE_{3z}}{dx} = -i\frac{\omega_3}{n_{3z}c}d(x)E_{1z}E_{2z}e^{i\Delta k_{SFG}x}. \quad (4)$$

Here, E, ω, n are electric field amplitude, angular frequency, and refractive index, respectively. Their subscripts $1, 2, 3$ denote FF_1, FF_2, and SF, respectively. $\beta(x) = -\gamma_{51}E_y n_{1y}^2 n_{1z}^2 f(x)$ with E_y be the applied transverse electric field, $d(x) = d_{33}f(x)$ is the modulated second-order nonlinear coefficient, $f(x)$ is the structural function of PPLN. d_{33} and γ_{51} are second-order nonlinear coefficient and electro-optic coefficient, respectively. c is the speed of light in the vacuum. $\Delta k_{EO} = k_{1y} - k_{1z}$ and $\Delta k_{SFG} = k_{1z} + k_{2z} - k_{3z}$ are the phase mismatches of EO polarization coupling and SFG process, respectively. Effective refractive indices in the ridge waveguide are used to calculate the wavevectors. $f(x)$ can be written as Fourier series: $f(x) = \sum_m g_m \exp(-iG_m x)$, where $G_m = 2m\pi/\Lambda$ is the reciprocal lattice vector (Λ is the poling period of PPLN and m is the order of QPM). g_m is the amplitude of reciprocal lattice vector. Thus, QPM SFG and EO processes can be easily simulated from the simplified coupled equations.

In the simulation, the length of ridge waveguide is 10 mm and its transverse width is 6 μm. Figure 1(a) shows the electric control capacity of the cascading process. Under the applied

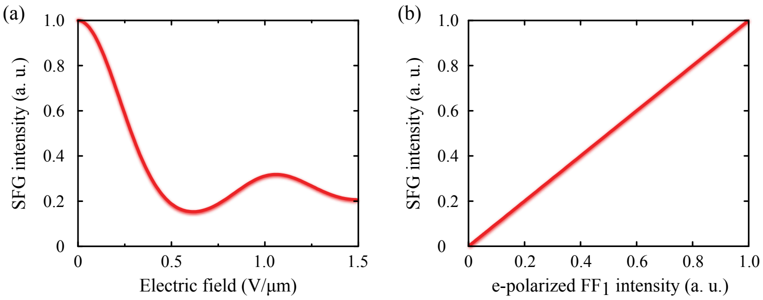

Fig. 1. (a) Simulation of SF^e output related to the applied electric field. (b) Intensity of SF^e with respect to the intensity of one fundamental wave (FF_1^e), with the other kept constant.

transverse electric field, one e-polarized fundamental wave transforms into o-polarized wave ($FF_1^e \rightarrow FF_1^o$), gradually decreasing the intensity of SFG ($FF_1^e + FF_2^e \rightarrow SF^e$). When the voltage further increases, the energy of o-polarized wave couples back to e-polarized wave and the intensity of SFG increases. The electric control capacity is satisfying according to the simulation. What is more, the drive voltage is low due to the enhancement of SFG and EO effect in the ridge waveguide. To verify the energy relation between SFG and fundamental waves, we simulate the intensity of SF^e with respect to the intensity of e-polarized fundamental wave (FF_1^e) showing linear relation, as shown in Fig. 1(b).

3. Experiment and discussion

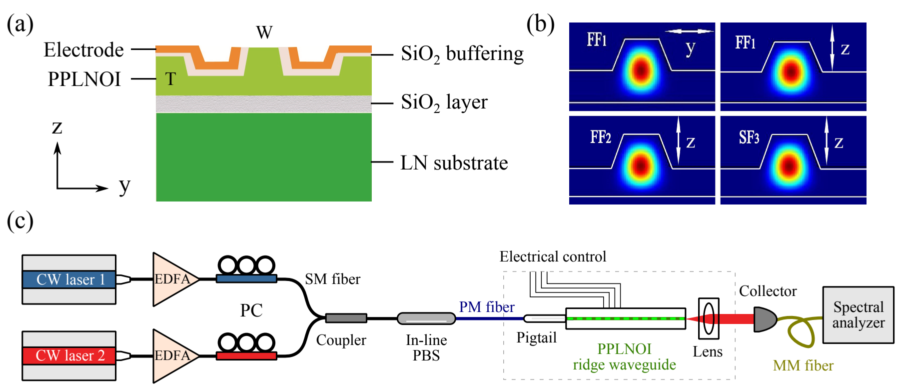

Fig. 2. (a) Cross-section structure of the PPLNOI ridge waveguide. (b) Simulated spatial fundamental mode profiles of each wave in the ridge waveguide. FF is in the telecom band (1550 nm) and SF is in the NIR range (775 nm). (c) Schematic illustration of the experimental setup.

In the experiment, we used a PPLNOI ridge waveguide (HC Photonics, Co.) to investigate dynamics of the SFG and EO process. Figure 2(a) shows the cross-section view of the PPLNOI ridge waveguide whose dimension is $6.0\ \mu m(W) \times 5.0\ \mu m(T) \times 10\ mm$. The waveguide with an approximately 2.6 μm high ridge is fabricated by optical grade dicing. The optical axis is along the z axis. The upper and lower surfaces of PPLN are coated with silica to form high refractive index difference. Light transmitted along the x axis in the ridge waveguide is tightly confined. Metallic electrodes (Ni/Cr) are plated onto the ridge waveguide to provide a transverse applied electric field (y-axis). The poling period of PPLN is 20.5 μm corresponding to QPM wavelength at telecom band and the duty cycle is 50%. The geometry is the same in our previous reports [16, 20]. Figure 2(b) shows the calculated fundamental spatial mode profiles of each wave, which shows good light confinement and also large mode overlapping. The mode-field diameters are about 4.6 μm. The confinement is between that in proton exchanged waveguides and nanophotonic ones. It should be noted that the waveguide is multi-mode, sustaining two spatial orders in telecom band and much more in the short wavelengths.

The experimental setup is depicted in Fig. 2(c). Light from two tunable continuous (CW) lasers (1520-1600 nm) separately amplified by an erbium-doped optical fiber amplifier (EDFA) is used as the fundamental waves, respectively. Polarization controllers (PCs) are used to guarantee their polarization. Light waves are combined by a 50×50 fiber coupler and then injected into the integrated waveguide device. The device includes a in-line polarized beam splitter (PBS) and polarization maintaining (PM) optical fiber, a PPLNOI ridge waveguide, electrical components and a temperature controller with an accuracy of $0.1°C$. The output light from the waveguide is collimated by a short focal length lens in free space. Then free space light is collected by using a collector and multimode fiber to be analyzed by a spectroscope.

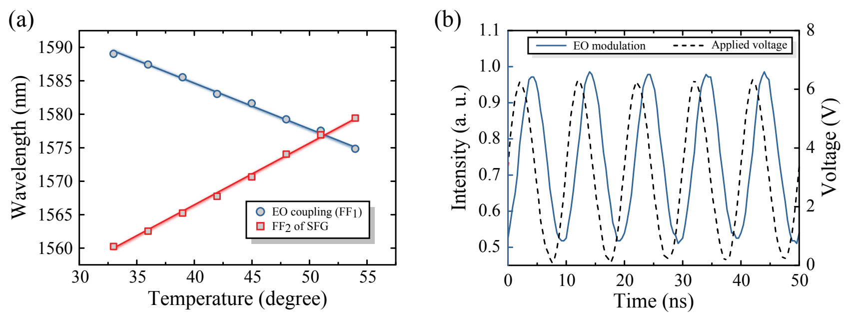

Fig. 3. (a) The temperature tuning of EO polarization coupling and SFG processes. (b) Experimental modulation of EO polarization coupling at a fast speed of 100 MHz.

Firstly, we replaced the optical fiber collector and spectroscope with an orthogonal polarizer and power meter to carry out EO polarization coupling experiment with only FF_1^e input. The matching relation of EO polarization coupling is shown in Fig. 3(a). The slope of linear fitting is $-0.67\ nm/°C$. The matching wavelength can be tuned by temperature in a wide range. We also measured the fast-speed modulation rate of EO polarization coupling by applying a sinusoidal voltage (small-signal) at a frequency of 100 MHz, as shown in Fig. 3(b). The applied signal is smaller than the half-wave voltage (13 V) limited by electrical equipment. The output light is dynamically modulated without moderate distortion at high frequency, showing that our experimental device can provide a fast-speed and stable response.

Then, we test the QPM conditions of SFG in the PPLNOI ridge waveguide. We injected both e-polarized fundamental waves to generate e-polarized SF light ($FF_1^e + FF_2^e \rightarrow SF^e$), utilizing the largest nonlinear coefficient (d_{33}). Since we only deal with e-polarization light during the experiment, the superscripts are some times dropped without ambiguity. We determined the cascading conditions by matching FF_2 wavelengths with FF_1 at EO polarization coupling, as shown in Fig. 3(a). As can be seen, the cascading can be achieved in a flexible manner working at different wavelengths. This is more advantageous than the cascading of EO polarization coupling and SHG [16], for which we also found a better experimental condition at approximately 1577 nm at $53°C$. In the case of $T = 42°C$ and $FF_1 = 1583.3\ nm$, Fig. 4(a) shows the SFG intensity relationship ($sinc$ function shaped) with respect to the wavelength of FF_2. The experimental central wavelength ($FF_2 = 1567.7\ nm$) agrees with theory ($FF_2 = 1567.8\ nm$). In our experiment, the SFG phase matching has a narrow bandwidth because we used type-0 QPM condition. The full-width at half-maximum (FWHM) of the phase matching spectrum

Optics EXPRESS

is 1.3 nm. In addition, we measured the relative intensity of SFG by altering the input power of FF_1. As shown in Fig. 4(b), the relationship between SFG and FF_1 is near linear since the intensity of SF is proportional to the product of intensities of two fundamental frequency waves $[I_{SF} \propto I_{FF_1} I_{FF_2} sinc^2(\Delta k_{SFG} L/2)]$, where Δk_{SF} is the phase mismatching of SFG process and L is the interaction distance. The calculated conversion efficiency is approximately $10^{-4}/W \cdot cm^2$, the same scale in our previous report of SHG and EO coupling cascading scheme [16].

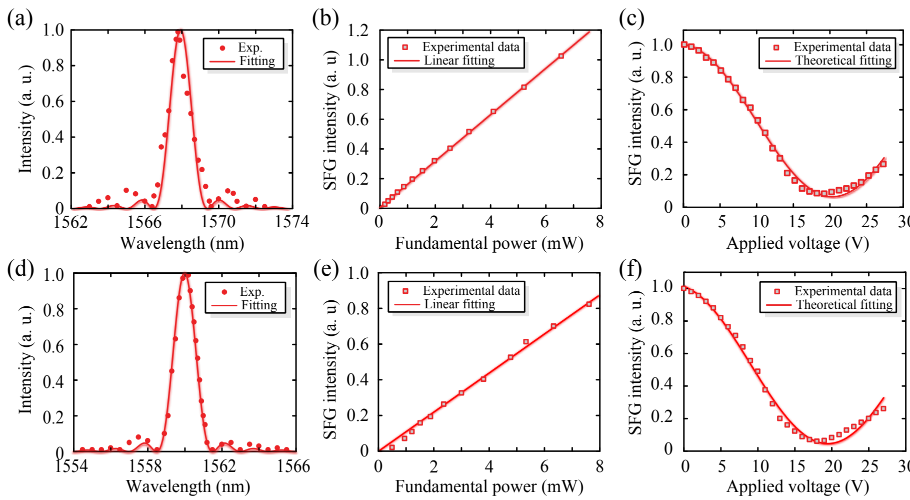

Fig. 4. (a) SFG efficiency versus FF_2 wavelength as $T = 42°C$ and $FF_1 = 1583.3\ nm$. (b) Linear relationship between intensity of SFG and input power of FF_1, while the power of FF_2 is fixed. (c) Intensity of SF varied with the applied voltage. The wavelength of $FF_2 = 1567.7\ nm$. (d,e,f) correspond to the situation when $T = 33°C$ and $FF_1 = 1589.0\ nm$.

To demonstrate the electrical manipulating capacity of the cascading process, we applied an electric field to invoke the EO polarization coupling and monitored the intensity of SF. Figure 4(c) shows the measured SFG intensity versus the applied voltage. The variation tendency is in accordance with theoretical simulation. At the beginning, with the increase of the applied voltage, a portion of z-polarized fundamental wave changes to y-polarized wave because of EO polarization coupling process ($FF_1^e \rightarrow FF_1^o$) and the intensity of SF gradually decreases. When further increasing the applied voltage, the energy of y-polarized wave couples back to the z-polarized fundamental wave ($FF_1^e \rightarrow FF_1^o \rightarrow FF_1^e$). As a result, the intensity of SF gradually increases. Obviously, the intensity of SF is successfully modulated by the applied electric field and as can be seen only a relatively low voltage is needed. Both the nonlinear wave mixing and electric field per voltage is obtained due to the PPLNOI ridge waveguide. This makes devices on the LNOI platform superior than their conventional bulk counterparts.

Beside, we also investigated these characteristics at different conditions, as the processes of EO polarization coupling and SFG are relative independent. Figures 4(d-f) correspond to the situation at $T = 33°C$ and $FF_1 = 1589.0\ nm$. Correspondingly, $FF_2 = 1560.2\ nm$ was used during the experiment. The same controlling dynamics was obtained. This proves that the configuration of SFG and EO polarization cascading is able to work on different wavelengths, thus unleashes the constraint on the input light. This holds more promise in real applications in integrated nonlinear photonics. Moreover, one can also obtain more cascading processes by exploiting phase mismatched EO polarization coupling and SFG (i.e., $\Delta k_1 = 0, \Delta k_2 \neq 0$; $\Delta k_1 \neq 0, \Delta k_2 = 0$; $\Delta k_1 \neq 0, \Delta k_2 \neq 0$). These cascading schemes would also provide more flexible ways for phase shift generation, multiwavelength frequency conversion and all-optical control.

4. Conclusion

In conclusion, frequency conversion and polarization coupling has been achieved simultaneously on a single LNOI chip. We succeeded to manipulate the intensity of SFG via EO polarization coupling by taking the advantage of the cascading process in a PPLNOI ridge waveguide. Both the driving voltage and input power is low due to enhancement on the LNOI platform. As the conditions of SFG and EO polarization coupling are relatively independent, the current configuration is flexible and operational at a wide wavelength range. The scheme will find applications in integrated electro-optical modulator, nonlinear optical processing, etc.

Funding

National Natural Science Foundation of China (NSFC) (11604206, 11734011); National Key R&D Program of China (2018YFA0306301, 2017YFA0303701); Foundation for Development of Science and Technology of Shanghai (17JC1400400).

References

1. G. I. Stegeman, D. J. Hagan, and L. Torner, "$\chi^{(2)}$ cascading phenomena and their applications to all-optical signal processing, mode-locking, pulse compression and solitons," Opt. Quantum Electron. **28**, 1691–1740 (1996).
2. A. Kobyakov and F. Lederer, "Cascading of quadratic nonlinearities: An analytical study," Phys. Rev. A **54**, 3455–3471 (1996).
3. C. Langrock, S. Kumar, J. E. McGeehan, A. E. Willner, and M. M. Fejer, "All-optical signal processing using $\chi^{(2)}$ nonlinearities in guided-wave devices," J. Light. Technol. **24**, 2579–2592 (2006).
4. G. I. Stegeman, M. Sheik-Bahae, E. V. Stryland, and G. Assanto, "Large nonlinear phase shifts in second-order nonlinear-optical processes," Opt. Lett. **18**, 13–15 (1993).
5. A. V. Buryak, P. D. Trapani, D. V. Skryabin, and S. Trillo, "Optical solitons due to quadratic nonlinearities: from basic physics to futuristic applications," Phys. Reports **370**, 63 – 235 (2002).
6. M. Ahlawat, A. Tehranchi, K. Pandiyan, M. Cha, and R. Kashyap, "Tunable all-optical wavelength broadcasting in a ppln with multiple qpm peaks," Opt. Express **20**, 27425–27433 (2012).
7. S. Ashihara, T. Shimura, K. Kuroda, N. E. Yu, S. Kurimura, K. Kitamura, M. Cha, and T. Taira, "Optical pulse compression using cascaded quadratic nonlinearities in periodically poled lithium niobate," Appl. Phys. Lett. **84**, 1055–1057 (2004).
8. J. Wang, J. Sun, C. Luo, and Q. Sun, "Experimental demonstration of wavelength conversion between ps-pulses based on cascaded sum- and difference frequency generation (sfg+dfg) in $linbo_3$ waveguides," Opt. Express **13**, 7405–7414 (2005).
9. G. S. Kanter, P. Kumar, K. R. Parameswaran, and M. M. Fejer, "Wavelength-selective pulsed all-optical switching based on cascaded second-order nonlinearity in a periodically poled lithium-niobate waveguide," IEEE Photonics Technol. Lett. **13**, 341–343 (2001).
10. J. Huo and X. Chen, "Large phase shift via polarization-coupling cascading," Opt. Express **20**, 13419–13424 (2012).
11. J. Huo, Y. Zheng, and X. Chen, "Active control of light based on polarization-coupling cascading," Appl. Phys. B **117**, 19–23 (2014).
12. M. Wang, Y. Xu, Z. Fang, Y. Liao, P. Wang, W. Chu, L. Qiao, J. Lin, W. Fang, and Y. Cheng, "On-chip electro-optic tuning of a lithium niobate microresonator with integrated in-plane microelectrodes," Opt. Express **25**, 124–129 (2017).
13. C.-P. Huang, Q.-J. Wang, and Y.-Y. Zhu, "Cascaded frequency doubling and electro-optic coupling in a single optical superlattice," Appl. Phys. B **80**, 741–744 (2005).
14. J.-W. Zhao, C.-P. Huang, Z.-Q. Shen, Y.-H. Liu, L. Fan, and Y.-Y. Zhu, "Simultaneous harmonic generation and polarization control in an optical superlattice," Appl. Phys. B **99**, 673–677 (2010).
15. Y. Kong, X. Chen, and T. Zhu, "Intensity modulation on polarization coupling and frequency conversion in periodically poled lithium niobate," Appl. Phys. B **102**, 101–107 (2011).
16. T. Ding, Y. Zheng, and X. Chen, "Integration of cascaded electro-optic and nonlinear processes on a lithium niobate on insulator chip," Opt. Lett. **37**, 1296–1300 (2019).
17. A. Boes, B. Corcoran, L. Chang, J. Bowers, and A. Mitchell, "Status and potential of lithium niobate on insulator (lnoi) for photonic integrated circuits," Laser & Photonics Rev. **12**, 1700256 (2018).
18. C. Wang, M. Zhang, X. Chen, M. Bertrand, A. Shams-Ansari, S. Chandrasekhar, P. Winzer, and M. LonXiang ar, "Integrated lithium niobate electro-optic modulators operating at cmos-compatible voltages," Nature **562**, 101–104 (2018).
19. C. Wang, M. Zhang, B. Stern, M. Lipson, and M. Lončar, "Nanophotonic lithium niobate electro-optic modulators," Opt. Express **26**, 1547–1555 (2018).
20. T. Ding, Y. Zheng, and X. Chen, "On-chip solc-type polarization control and wavelength filtering utilizing periodically poled lithium niobate on insulator ridge waveguide," J. Light. Technol. **37**, 1296–1300 (2019).